

# Growth diversity in one dimensional fluctuating interfaces

M. D. Grynberg

Departamento de Física, Universidad Nacional de La Plata  
C.C. 67, (1900) La Plata, Argentina

## Abstract

A set of one dimensional interfaces involving attachment and detachment of  $k$ -particle neighbors is studied numerically using both large scale simulations and finite size scaling analysis. A labeling algorithm introduced by Barma and Dhar in related spin Hamiltonians enables to characterize the asymptotic behavior of the interface width according to the initial state of the substrate. For equal deposition–evaporation probability rates it is found that in most cases the initial conditions induce regimes of saturated width. In turn, scaling exponents obtained for initially flat interfaces indicate power law growths which depend on  $k$ . In contrast, for unequal probability rates the interface width exhibits a logarithmic growth for all  $k > 1$  regardless of the initial state of the substrate.

PACS numbers: 05.40.-a, 05.70.Ln, 64.60.Ht

**KEY WORDS:** irreducible string; saturated regimes; logarithmic growth.

Published in J. STAT. PHYS. **103**, 395 (2001).

Studies of interface growth have acquired a major momentum in the past decade [1, 2, 3], finding a rich variety of applications. These range from molecular beam epitaxy [4] to magnetic flux lines in type-II superconductors [1, 5] and polymer physics [6]. Most numerical analysis and theoretical investigations on growing structures have emphasized the onset of scaling regimes which emerge at both large time and length scales. This enables a classification of nonequilibrium interfaces by universality classes characterized by a set of scaling exponents which, independently of the microscopic growth rules, dominate the late evolution stages of these processes.

However, the issue of universality classes in these problems has been steadily brought into question, particularly in higher dimensions [7, 8, 9, 10]. Since no systematic analytical method is yet available to understand large scale fluctuations in nonequilibrium systems, two main research lines have been addressed to probe the universality hypothesis. They involve either the simulation of discrete models [10, 11, 12, 13, 14] or the numerical solution of phenomenological Langevin-type equations of growth driven by Gaussian noise [16]. This is the case of the ubiquitous Kardar-Parisi-Zhang (KPZ) equation [17] which has been applied to characterize a vast body of far from equilibrium processes [1, 2, 3].

In this letter we rather follow the first category of investigations and introduce a set of restricted solid-on-solid (RSOS) growth models in one dimension entailing an exceptionally large number of conservation laws [18]. By mapping the problem onto a quantum spin system, it will turn out that for equilibrium situations, not only each model defines a “class” of its own but furthermore, their asymptotic properties become extremely sensitive to slight deviations from initially flat substrates. In contrast, non-equilibrium situations are rather robust but exhibit a much slower dynamics. This will mark a clear difference between fluctuations in equilibrium and non-equilibrium cases.

The basic process considered is a simple yet nontrivial extension of ballistic aggregation models [14]. Here, we include both deposition and evaporation of extended objects such as dimers, trimers, ...  $k$ -mers, at random locations of a one-dimensional interface [15]. As usual, the state of the system at a given time is defined by a set of single valued functions  $\{h_1(t), \dots, h_L(t)\}$ , where  $h_n$  is the height of the interface measured from a reference level at site  $n \in \{1, 2, \dots, L\}$ . To prevent the divergence of surface fluctuations at large times we also impose a RSOS constraint throughout the

process namely,  $|h_{n+1} - h_n| \equiv 1, \forall t$ . Therefore, a  $k$ -mer deposition (evaporation) attempt with rate  $\epsilon$  ( $\epsilon'$ ) is successful provided a plateau with at least  $k$ -successive local minima (maxima) is selected from the interface. Fig. 1 illustrates these microscopic rules for the case of dimers. Notice that evaporation apply whether or not the targeted  $k$ -adjacent maxima were created together, a feature which allows for reconstitution of  $k$ -mers. Also, it is helpful pointing out that the dynamics of these interfaces is equivalent to that defined in the  $2k$ -mer deposition-evaporation problem studied in Ref. [18], by flipping the spins on all even sites, say, of this latter system.

In studying the scaling regimes of growing structures it is useful to consider the mean square fluctuations  $W^2$  of the average interface height  $\langle h(t) \rangle$ , i.e.  $W^2(L, t) = \frac{1}{L} \sum_j \langle [h_j(t) - \langle h(t) \rangle]^2 \rangle$ , which yields a measure of the interface width. From the assumption of a scaling form of height-height correlation functions along with a single time-dependent length scale  $\sim t^{1/z}$  for growth starting from an initially flat interface, it can be argued [19] that  $W$  scales as

$$W(L, t) = L^\zeta f(t/L^z), \quad (1)$$

where the scaling function  $f(c)$  satisfies

$$f(c) \sim \begin{cases} c^{\zeta/z} & \text{for } c \ll 1, \\ \text{const} & \text{for } c \gg 1. \end{cases} \quad (2)$$

It follows immediately that finite systems saturate as  $W \propto L^\zeta$ , whereas in the thermodynamic limit the asymptotic growth is dominated by the exponent  $\beta = \zeta/z$ , that is  $W \propto t^\beta$ . The exponent  $\zeta$  describes the roughness dependence of the surface width on the typical substrate size. In turn the exponent  $z$ , often known as the dynamic exponent, gives the fundamental scaling between length and time.

However, already for  $k \geq 2$  it will turn out that there are initial substrates whose asymptotic widths neither follow a power law nor exhibit the universal characteristics embodied in Eqs. (1) and (2). As we shall see, the investigation of these issues becomes rather systematic in the language of the spin systems discussed below.

*a. Spin representation* — We now exploit the well known mapping between RSOS interface dynamics and quantum spin systems [14]. Associating the height difference  $s_n \equiv h_{n+1} - h_n$  to an eigenvalue of the  $z$ -component, say, of the Pauli operator  $\vec{\sigma}_n$  for site  $n$ , then all intrinsic properties of the interface can be analyzed in

terms of direct products  $|s\rangle = |s_1, \dots, s_L\rangle$  of  $1/2$  spinors. By construction it is clear that up to a constant, the interface heights are obtained as  $h_n = h_1 + \sum_{j=1}^{n-1} s_j$ , where  $h_1 - h_L = s_1$  upon imposing periodic boundary conditions (PBC). Note that the latter force a vanishing total magnetization throughout the underlying spin kinetics.

Introducing spin- $1/2$  raising and lowering operators  $\sigma_n^+$ ,  $\sigma_n^-$ , the stochastic evolution of our  $k$ -mer interfaces at subsequent times can be calculated from the action  $e^{-Ht}$  of the quantum ‘‘Hamiltonian’’

$$H = \sum_j \left( \epsilon A_j^\dagger + \epsilon' A_j \right) \left( A_j^\dagger + A_j - 1 \right), \quad (3)$$

$$A_j^\dagger = \prod_{i=1}^k \sigma_{j+2i-2}^+ \sigma_{j+2i-1}^-. \quad (4)$$

Here, adsorption (desorption) of  $k$ -mer plateaus with probability  $\epsilon$  ( $\epsilon'$ ) is described by the effect of the  $A^\dagger$  ( $A$ ) operators. Conservation of probability requires in turn the appearance of  $2k$ -field correlators, already diagonal in the  $\sigma^z$  or particle (monomer) representation. We address the reader to Ref. [20] for a more detailed derivation in related systems.

*b. Conservation laws* — The advantage of the spin representation is that one can identify a large number of subspaces which are mutually disconnected by the  $H$ -dynamics. Following Ref.[18], we define accordingly a reduction rule by looking for the occurrence of groups of  $2k$ -opposite *consecutive* spins in a given state  $|s\rangle$ . Each occurrence, if any, is deleted so the length of the remaining spin configuration is reduced in  $2k$  bits per deletion. This procedure is applied recursively, until we are left with a string that cannot be further reduced. Such an object corresponds to an *irreducible string*  $I|s\rangle$  [18]. For example, in the dimer case we have  $I|\uparrow\uparrow\downarrow\downarrow\uparrow\downarrow\downarrow\uparrow\rangle = \uparrow\uparrow\downarrow\downarrow\uparrow\downarrow\downarrow\uparrow$  (irreducible block of Fig. 1),  $I|\uparrow\downarrow\uparrow\downarrow\uparrow\downarrow\uparrow\rangle = \uparrow\downarrow\uparrow$ ,  $I|\uparrow\downarrow\uparrow\downarrow\uparrow\downarrow\uparrow\rangle = \emptyset$ , the null string.

The key observation is that so long as  $\epsilon, \epsilon' > 0$ , two spin configurations  $|s\rangle$  and  $|s'\rangle$  belong to the same subspace  $\iff I|s\rangle = I|s'\rangle$  [18]. Thus, treated as a dynamical variable, the irreducible string is a constant of motion and provides a unique label for each  $H$ -invariant subspace. To illustrate this point consider a sector labeled by  $\chi_1, \dots, \chi_{\mathcal{L}}$  with  $\mathcal{L} < L$  irreducible characters  $\chi = \pm 1$ . Let  $\{x_j(t)\}$  denote their positions in the full  $L$ -site lattice before applying the reduction rule. The interface dynamics then induces a random walk of these characters such that

$x_{j+1}(t) > x_j(t) \forall t$ . Since  $H$  changes  $x_j$  by multiples of  $2k$  lattice spacings, the spin array between sites  $x_j$  and  $x_{j+1}$  can be ultimately reduced to a null string. Thus, we see that  $\{x_j(t)\}$  constitute the slow modes of our fluctuating interfaces whereas their characters remain unaltered throughout the dynamics. The above reduction algorithm also enables to count the total number of invariant sectors, both jammed (strings which are already irreducible), and unjammed. A straightforward analysis given as in [18] shows that these sectors increase as fast as  $\lambda^L$  for large  $L$ , where  $\lambda$  is the largest root of  $\lambda^{2k} = 2\lambda^{2k-1} - 1$ .

*c. Saturated regimes* — It is then natural to ask whether the dynamics is affected by this rather unusual partition of the full phase space. At least in the simpler case, when  $\epsilon = \epsilon'$  [21], it can be argued that  $W$  remains bounded whenever we start from a substrate of finite width and the length  $\mathcal{L}$  of the corresponding irreducible string is a finite fraction of the lattice size. Specifically, consider two arbitrary points  $A$  and  $B$  in a ring of  $L$  sites. The most general configuration of spins determining the height difference  $h_A - h_B$  can be denoted as

$$u_1 \left| \overset{h_A}{x_1 w_1 x_2 w_2 \dots x_{n-1} w_{n-1} x_n} \right| \overset{h_B}{u_2},$$

where  $x_i$  are the positions of the irreducible characters between  $A$  and  $B$ ,  $w_i$  are spin patches reducible to null strings, and  $u_1$  ( $u_2$ ) is the part of the irreducible string between the previous (next) irreducible character  $x_0$  ( $x_{n+1}$ ) that lies to the left of  $A$  (right of  $B$ ). To calculate the height difference between  $A$  and  $B$ , we can ignore all  $w_i$  patches as they necessarily have equal number of up and down steps. On the other hand, if the initial substrate has bounded heights, the sequence  $x_1(t) \dots x_n(t)$  can only give a bounded contribution to the height difference  $\forall t$ . The remaining contributions at subsequent times comes from  $u_1$  and  $u_2$ . If  $u_1$  is part of a reducible substring of length  $2m$  (between  $x_0$  and  $x_1$ ), the maximum height difference it can have is at most  $m$ . Also, for  $\epsilon = \epsilon'$  the detailed balance condition holds in the steady state. For such equilibrium situation it has been shown that  $m$  has an exponential distribution, provided that the density  $\mathcal{L}/L$  of irreducible characters is held finite [18]. Consequently,  $u_1$  yields only a finite variance. Similar considerations apply to  $u_2$ . Hence, the height difference between two arbitrary points has bounded variance  $\forall t$  and  $L$ . Therefore, we conclude that the width of the substrate remains finite, or equivalently, in the steady state  $W$  should exhibit a saturated regime. However,

notice that if the irreducible string is very short, i.e.  $\mathcal{L}/L \rightarrow 0$ , fluctuations in the  $(x_{j+1} - x_j)$  distances become large and the above reasoning for  $u_1, u_2$  does not hold.

The case  $k = 2$  is typical and already exhibits such sector dependent behavior. Thus, we consider only this case in detail.

*d. Numerical results* — Armed with this labeling methodology along with the spin-height mapping discussed above, we studied the dimer interface width  $W$  in a number of representative subspaces. Fig. 2 displays the width behavior obtained from Monte Carlo simulations using five initial scenarios. These were embedded homogeneously on the Neel state of  $2.1 \times 10^5$  lattice sites with PBC, and correspond to (1) the null string, i.e. the usual flat substrate; (2)  $[\uparrow\uparrow\downarrow\downarrow]^{L/60}$  that is, the irreducible string constructed by repeating the unit cell  $L/60$  times; (3)  $[\uparrow\uparrow\downarrow\downarrow]^{L/8}$ ; (4)  $[\uparrow\uparrow\downarrow\downarrow\uparrow]^{L/14}$ ; (5) a random configuration formed by deposition-evaporation of monomers on the Neel state. Setting  $\epsilon = \epsilon'$ , the averages were taken over 100 histories of  $10^5$  steps per height.

Although for  $\epsilon = \epsilon'$  the interface of sector (1) moves on the average with zero velocity [see lower inset of Fig. 3(a)], alike the monomer case ( $k = 1$ ) it can grow to arbitrarily large heights. In fact, this is consistent with our data which support a power law growth  $W^2 \propto t^{2\beta}$  extended over more than two decades with an exponent  $\beta \sim 0.12(1)$ . On the other hand, sectors (3) and (4) clearly exhibit the saturated regimes conjectured above. They fit well with an exponential form  $W^2 \propto \exp(-t^{-\alpha})$ , as is shown in the semi-log inset of Fig. 2 upon setting  $\alpha \approx 1/4$  and  $1/3$  respectively [22], in sharp contrast with the expectations of Eqs.(1) and (2). Thus, we see that certain deviations from a perfectly flat substrate turn into drastic changes at large times. As it was referred to above, the latter depend on both the density  $\rho = \mathcal{L}/L$  and particular sequence of irreducible characters considered [23].

The situation of sectors (2) and (5) is less clear. Here  $\rho$  is still finite (though much smaller than the irreducible density of the previous non null sectors), and consequently a saturated regime would be expectable. However, also here the data extend nearly over two decades following power law growths with  $\beta \approx 0.07$  and  $0.04$  respectively (dashed slopes of Fig. 2). One may attempt to interpret these results in terms of a temporal crossover, although to reach an asymptotic saturated regime such a crossover should be exceptionally slow. A numerical test in favor of this latter possibility is provided by the average interface height  $\langle h(t) \rangle$ . Notice that

given a distribution of heights  $P(h_1, \dots, h_L, t)$ , the mean height can be evaluated as

$$\partial_t \langle h \rangle = \frac{4}{L} \sum_{|h\rangle, i} \epsilon P(\dots \overbrace{h_i^{(1)}, h_i, h_i^{(1)}, h_i, h_i^{(1)}}^{\text{dimer}} \dots, t) - \epsilon' P(\dots \overbrace{h_i^{(1)}, h_i^{(2)}, h_i^{(1)}, h_i^{(2)}, h_i^{(1)}}^{\text{dimer}} \dots, t), \quad (5)$$

where  $h_i^{(j)} = h_i + j$ , and the overbraces involve the heights which form a dimer, say  $h_{i-1}, \dots, h_{i+3}$  (see Fig. 1). For  $\epsilon = \epsilon'$ , it follows that  $\langle h(t) \rangle$  must saturate to a finite value at large times, as all accessible height configurations are equally likely in the steady state, *irrespective* of the sector considered [21]. In fact, Fig. 3 (a) displays saturation regimes in most sectors. However, it also reveals the existence of a rather huge temporal crossover in sector (2) (more than  $10^5$  steps), along with a medium one in sector (5) (about  $10^3$  steps), possibly responsible for the unexpected width behavior observed in Fig. 2. It is important to note that for  $\epsilon > \epsilon'$  the average interface height behaves quite differently, at least within our accessible time scales. The latter can grow indefinitely with a non zero velocity, as suggested by the asymptotic logarithmic increase of  $\langle h(t) \rangle$  observed in Fig. 3 (b) for all sectors.

Before discussing such logarithmic behavior (see section *e* below), we complete our study of the case  $\epsilon = \epsilon'$  and analyze the late growing stages of higher  $k$ -mer interfaces, now focusing attention on initially null strings, the common flat substrate. After averaging over 100 histories our results indicate a slight dependence of  $\beta$  on the value of  $k$  (however, see below the variation of  $z$ ), which nonetheless can be clearly distinguished over five step decades, as indicated by the slopes of Fig. 4. The measured values of  $\beta$  are presented in Table I for  $k = 2, 4$  and  $8$ .

To enable a complementary check of these exponents we turn to a finite size scaling analysis of the interface width. The reader's attention is directed to Figs. 5(a)-(c) where we display in turn the results of the simulations carried out for  $k = 2, 4$  and  $8$ . Here, the averages were taken over  $2 \times 10^4$  samples employing periodic chains of  $L = 400, 640$  and  $800$  sites. Using the estimates of the dynamic and roughening exponents  $\{z, \zeta\}$  given in Table I, we obtained a fair data collapse towards the (squared) phenomenological scaling functions conjectured by Eqs.(1) and (2) [19]. As expected, the resulting values of  $\zeta/z$  are in reasonable agreement with the previous  $\beta$ -set obtained in the thermodynamic limit. So we finally see that as long as the deposition-evaporation rates are held equal, the emerging scaling exponents are in fact nonstandard and give rise to rather unusual dynamic length scales  $t^{1/z}$

which decrease markedly with  $k$ .

*e. Logarithmic growth.*  $\epsilon \neq \epsilon'$  — The logarithmic dependence of the average interface height  $\langle h(t) \rangle$  obtained in Fig. 3(b) at large times, may be understood by means of the following heuristic considerations. For clarity of argument, assume  $\epsilon \gg \epsilon'$ . The random deposition leaves some single spaces between segments occupied by dimers. This single spaces cannot be filled by subsequent deposition of dimers, with the result that the height profile after many depositions resembles a “mountain landscape” where no further depositions are possible. Such profile is clearly evidenced by the evolution snapshot given in the upper panel of Fig. 6.

If  $\epsilon' = 0$ , this configuration cannot evolve any further, and the configuration is stuck. If  $\epsilon'$  is non-zero, one can evaporate away from one side of the mountain, all the way to the base, and then redeposit the base by dimer shifting it one unit (right or left, whatever is allowed). Then, rebuilding on this side, one gets a different profile (dotted line in the lower panel of Fig. 6). This rebuilding process leads to sometimes extinction of small mountains (which merge with bigger ones), and thus the average mountain size  $M(t)$  increases with time. The time dependence of  $M$  can be estimated as follows. For a single rearrangement event described above, one needs order  $M$  evaporation events. Hence by standard activation arguments, this rate is  $(\epsilon'/\epsilon)^M$ . One needs order  $M^2$  such events for total width to change by  $M$  (since change occurs either way). Hence, the time for the average mountain size to change from  $M$  to  $2M$  is of order  $M^2(\epsilon/\epsilon')^M$ , so we get  $t(2M) \sim M^2(\epsilon/\epsilon')^M$ . On the other hand, from simple geometry both the average mountain height and the width  $W$  scale as  $M$  (i.e. the roughness exponent  $\zeta$  is 1). Therefore, this yields

$$W(t) \sim \log(t), \quad \epsilon \neq \epsilon'. \quad (6)$$

These conclusions can be extended for all substrates (whatever the sector or irreducible string considered), as well as  $\forall k > 1$ . In fact, the semi-log data displayed in Fig. 7 corroborates the above conjecture for  $k = 2, 4$ , and 8 starting from empty substrates. Also, the upper inset confirms this logarithmic growth for  $k = 2$  in sectors (2)–(5). A similar one-dimensional model showing logarithmically slow coarsening was studied in [24].

To summarize, we have studied a family of simple growth models yet exhibiting highly nontrivial behavior. For  $\epsilon = \epsilon'$  our finite size analysis indicates that each



$k$ -mer process might be regarded as a growth class of its own dominated by different dynamic exponents  $z(k)$ . The large systems explored within the time scales of Fig. 4 yielded growth exponents consistent with the  $\beta$  values obtained from finite substrates (Fig. 5). The concept of irreducible string [18] played a crucial role in determining the saturated behavior entailed by the initial conditions (Fig. 2), as opposed to the much simpler dynamics of monomer interfaces. However, the late dynamic stages of small strings ( $\mathcal{L} \ll L$ ) involve slow temporal crossovers for which further numerical efforts will be required to clarify such situations. Generalizations of this labeling algorithm to higher dimensions are clearly desirable though its mere existence appears difficult to elucidate. Whether or not an exponential number of conservation laws show up in  $d > 1$  yet remains an open question.

For the non-equilibrium situation ( $\epsilon \neq \epsilon'$ ), Fig. 7. indicates a rather robust dynamics. Here, the interface width grows logarithmically  $\forall k > 1$  irrespective of the initial state of the substrate. In view of these drastic differences between fluctuations in equilibrium and non-equilibrium cases, the transient dynamics of regimes with  $\epsilon \approx \epsilon'$  still needs further investigations.

It is a pleasure to thank R.B. Stinchcombe, M. Barma and T.J. Newman for helpful comments. Also, the remarkable observations made by the referee contributed to improve this work. The author acknowledges support of CONICET, Argentina.

## References

- [1] J. Krug, Adv. Phys. **46**, 139 (1997); J. Krug and H. Spohn, in *Solids far from Equilibrium: Growth, Morphology and Defects*, edited by C. Godrèche (Cambridge University Press, Cambridge, 1995).
- [2] T. Halpin-Healy and Y.-C. Zhang, Phys. Rep. **254**, 215 (1995).
- [3] P. Meakin Phys. Rep. **235**, 189 (1993); P. Meakin in *Phase Transitions and Critical Phenomena*, edited by C. Domb and J. L. Lebowitz (Academic, New York, 1988), Vol. 12.
- [4] P. Politi, G. Grenet, A. Marty, A. Ponchet and J. Villain, Phys. Rep. **324**, 271 (2000); D. E. Wolf and J. Villain, Europhys. Lett. **13**, 389 (1990).

- [5] T. Hwa, Phys. Rev. Lett. **69**, 1552 (1992).
- [6] M. Kardar and Y. -C Zhang, Phys. Rev. Lett. **58**, 2087 (1987).
- [7] J. Krug, Phys. Rev. Lett. **72**, 2907 (1994).
- [8] T. J. Newman and M. R. Swift, Phys. Rev. Lett. **79**, 2261 (1997).
- [9] J. M. López, Phys. Rev. Lett. **83**, 4594 (1999).
- [10] H. M. Koduvely and D. Dhar, J. Stat. Phys. **90**, 57 (1998).
- [11] J. Kertész and D. E. Wolf, Phys. Rev. Lett. **62**, 2571 (1989).
- [12] T. Ala-Nissila, T. Hjelt, J.M. Kosterlitz and O. Venäläinen, J. Stat. Phys, **72**, 207 (1993).
- [13] B. M. Forrest and L.-H. Tang, Phys. Rev. Lett. **64**, 1405 (1990).
- [14] P. Meakin, P. Ramanlal, L.M. Sander and R.C. Ball, Phys. Rev. A **34**, 5091 (1986); M. Plischke, Z. Rácz and D. Liu, Phys. Rev. B **35**, 3485 (1987).
- [15] Related growth process involving dimers were introduced recently by H. Hinrichsen and G. Ódor, Phys. Rev. Lett. **82**, 1205 (1999); H. Hinrichsen and G. Ódor, Phys. Rev. E **60**, 3842 (1999); J. D. Noh, H. Park and M. den Nijs, Phys. Rev. Lett. **84**, 3891 (2000).
- [16] J. G. Amar and F. Family, Phys. Rev. A **41**, 3399 (1990); K. Moser and D. E. Wolf, J. Phys. A **27**, 4049 (1994).
- [17] M. Kardar, G. Parisi, and Y.-C. Zhang, Phys. Rev. Lett. **56**, 889 (1986).
- [18] M. Barma and D. Dhar, Phys. Rev. Lett. **73**, 2135 (1994); D. Dhar and M. Barma, Pramana **41**, L193 (1993); M. Barma in, *Nonequilibrium Statistical Mechanics in One Dimension*, edited by V. Privman, (Cambridge University Press, 1996); R.B. Stinchcombe, M.D. Grynberg and M. Barma, Phys. Rev. E **47**, 4018 (1993).
- [19] F. Family and T. Vicsek, J. Phys. A **18**, L75 (1985).

- [20] G. M. Schütz, in *Phase Transitions and Critical Phenomena*, edited by C. Domb and J. L. Lebowitz, (Academic, London 2000); M. D. Grynberg and R. B. Stinchcombe, Phys. Rev. E **61**, 324 (2000).
- [21] For  $\epsilon = \epsilon'$ ,  $H$  is a self adjoint stochastic operator. Hence, the steady state of a given subspace is an equally weighted sum of all reachable configurations and therefore detailed balance holds.
- [22] Naturally, for large times and  $\alpha > 0$  this is equivalent to the simpler form  $A - B/t^\alpha$ . However, the best fit corresponds to the exponential form referred to above, implying that higher order corrections become relevant within our accessible time scales.
- [23] However, PBC impose the constraint  $\sum_{n=1}^{\mathcal{L}} \chi_n = 0$ .
- [24] M.R. Evans, Y. Kafri, H.M. Koduvvely and D. Mukamel, Phys. Rev. E **58**, 2764 (1998).

$k$	$\beta (L \rightarrow \infty)$	$z$	$\zeta$
2	0.12(1)	2.5(10)	0.3(1)
4	0.10(1)	2.8(10)	0.3(1)
8	0.09(1)	3.3(10)	0.3(1)

Table 1: Growth exponent  $\beta$  measured in large  $k$ -mer substrates (Fig. 4), along with finite size scaling estimations of dynamic and roughening exponents  $z$  and  $\zeta$  (Fig. 5), obtained for equal deposition–evaporation rates.

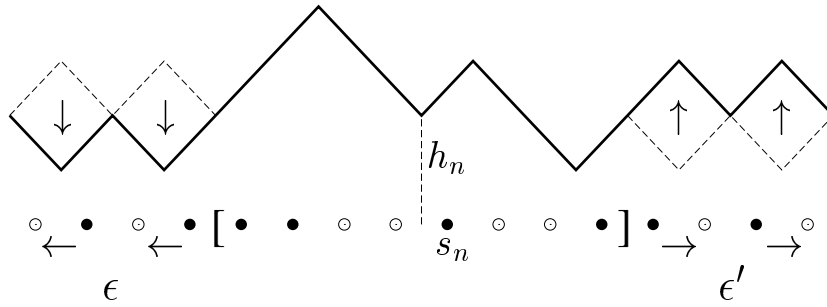


Figure 1: Schematic representation of dimer deposition- evaporation onto a RSOS interface. The equivalent spin- $\frac{1}{2}$  ( $s_n \equiv h_{n+1} - h_n$ ), or hard core particle dynamics involves two left (right) particle hopping at a time with rate  $\epsilon$  ( $\epsilon'$ ) for dimer adsorption (desorption). The array between brackets illustrates an irreducible string (see text).

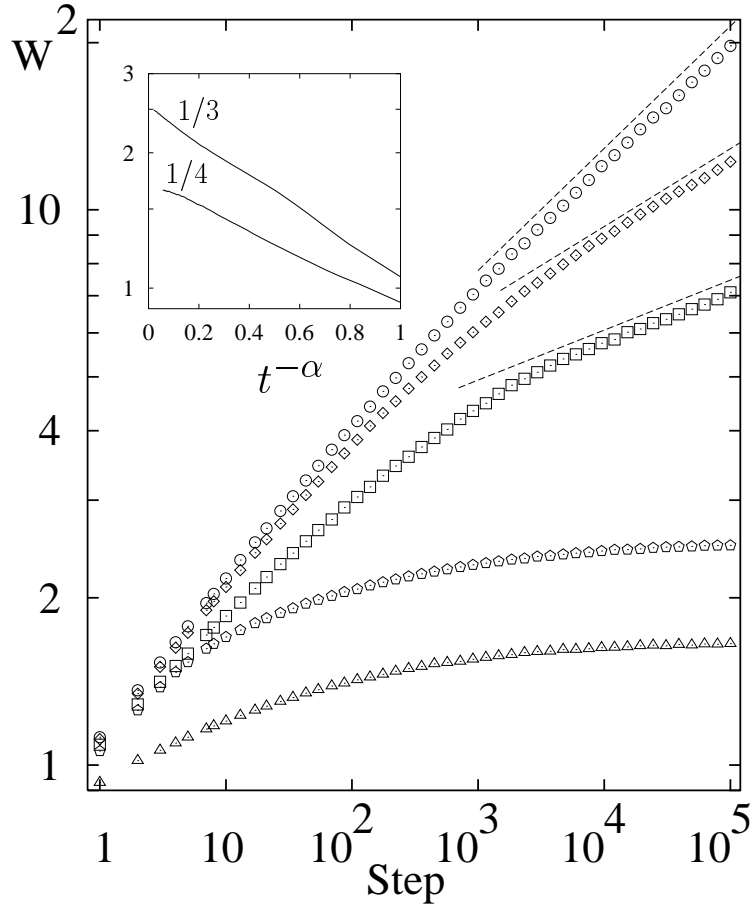
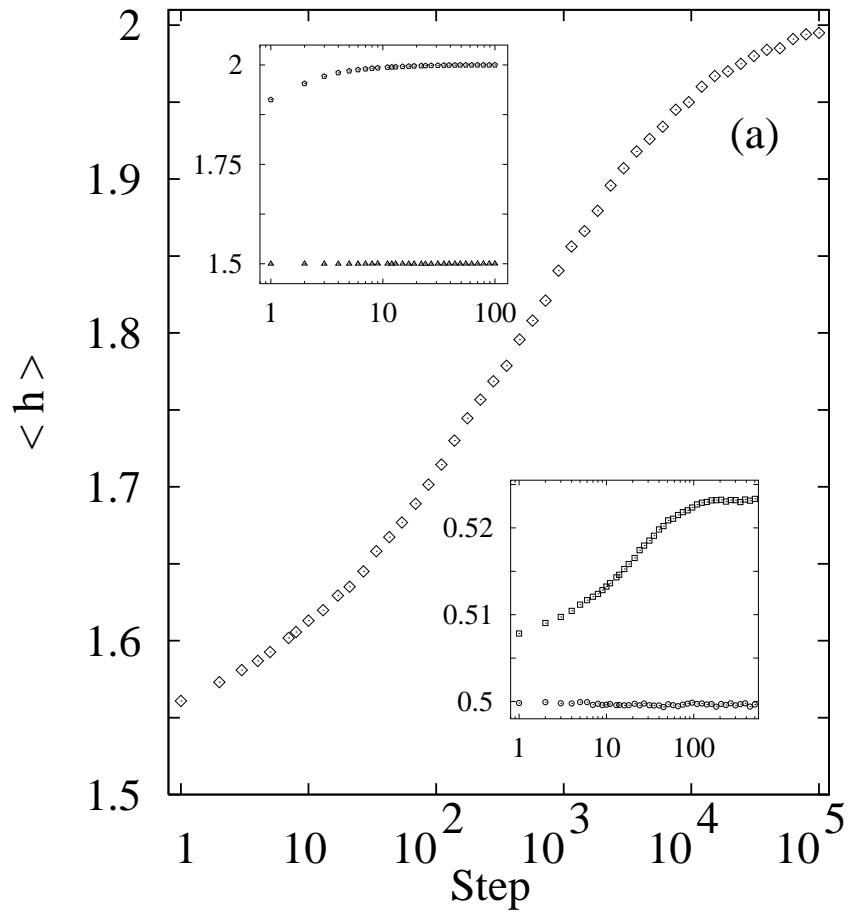


Figure 2: Evolution of  $W^2$  in subspaces (1)-(5) defined in text. Here, they correspond to (1) circles (null string); (2) rombooids; (3) triangles; (4) pentagons and; (5) squares. The slopes of upper straight lines indicate a power-law asymptotic behavior  $t^{2\beta}$  with  $\beta \approx 0.12$  (top),  $0.07$  (middle),  $0.04$  (bottom). These two latter cases however, might be undergoing a slow temporal crossover (see text). In turn, subspaces (3) and (4) fit appropriately an exponential form  $W^2 \propto \exp(-t^{-\alpha})$  with  $\alpha \approx 1/4$  and  $1/3$  respectively, as shown in the inset.



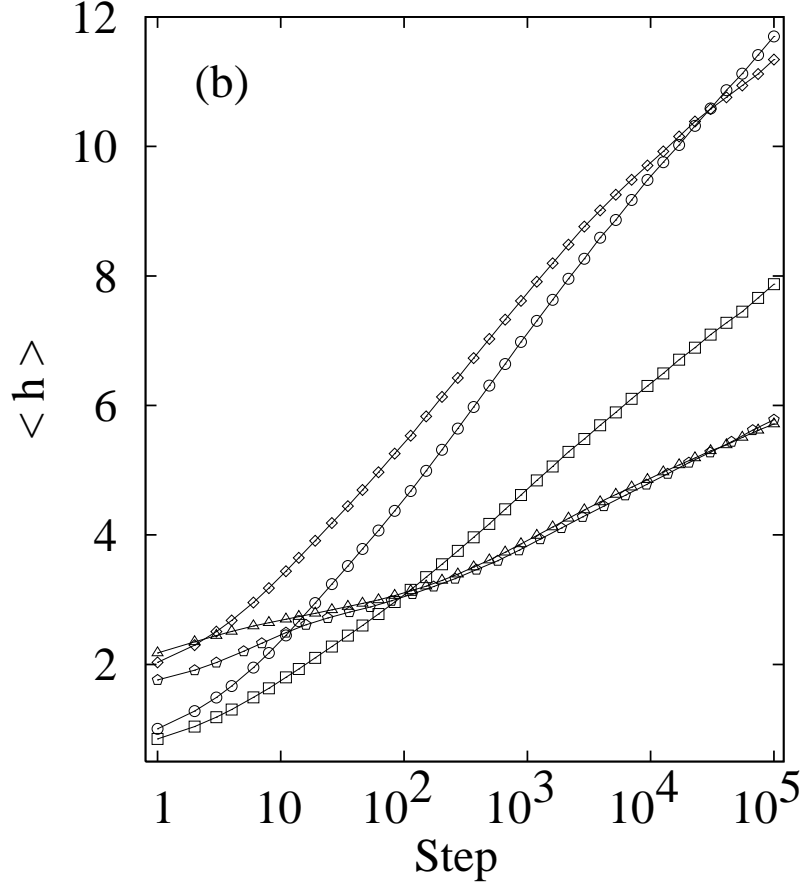


Figure 3: Average interface height  $\langle h \rangle$  for  $k = 2$  with (a)  $\epsilon = \epsilon'$ , measured from the flat interface level [ $\langle h(0) \rangle = 0.5$ ]. Sectors (1) (bottom curve of lower inset), (4) and (3) (from top to bottom in the upper inset), display a fast relaxation toward the expected saturated regime. In contrast, sectors (2) (romboids) and (5) (top curve of lower inset), undergo a slow temporal crossover. (b) Average height  $\langle h \rangle$  for  $k = 2$  with  $\epsilon'/\epsilon = 0.4$ . All sectors exhibit logarithmic growth at large times as opposed to the saturated regimes in (a). Solid lines are guide to the eye whereas all symbols are taken as in Fig. 2.

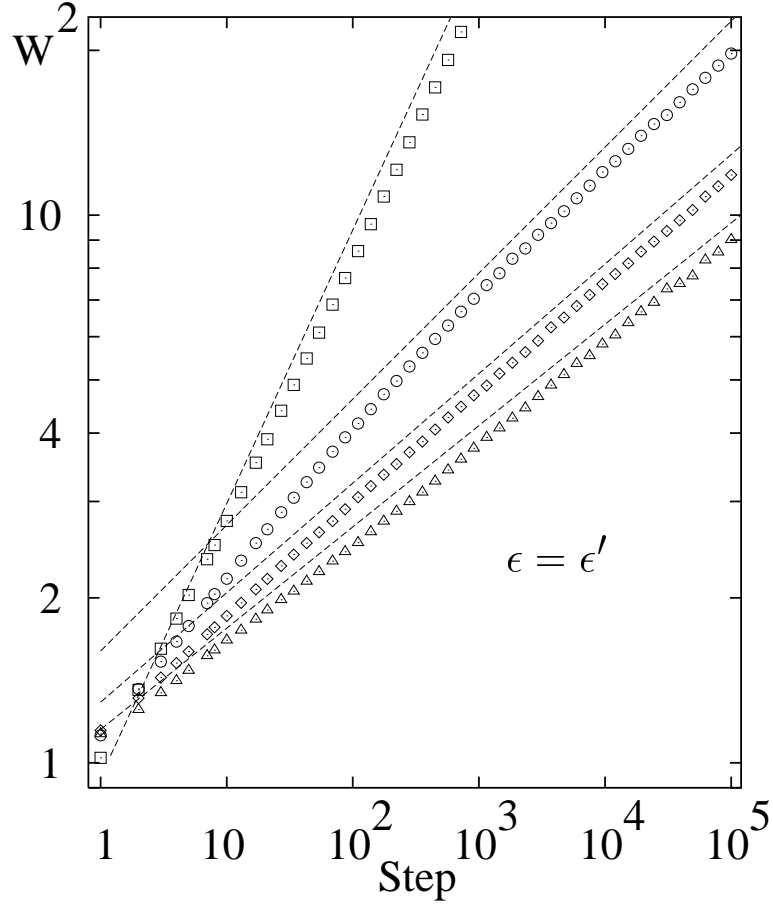
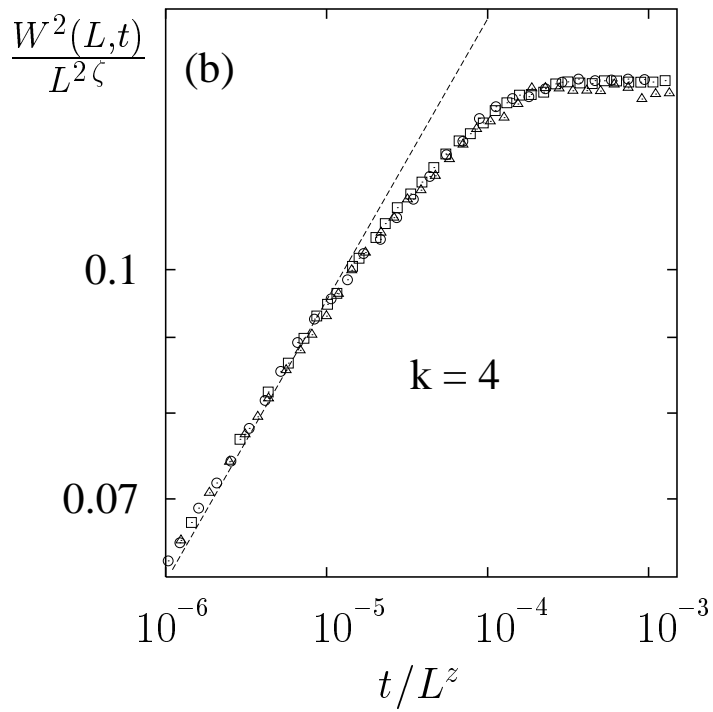
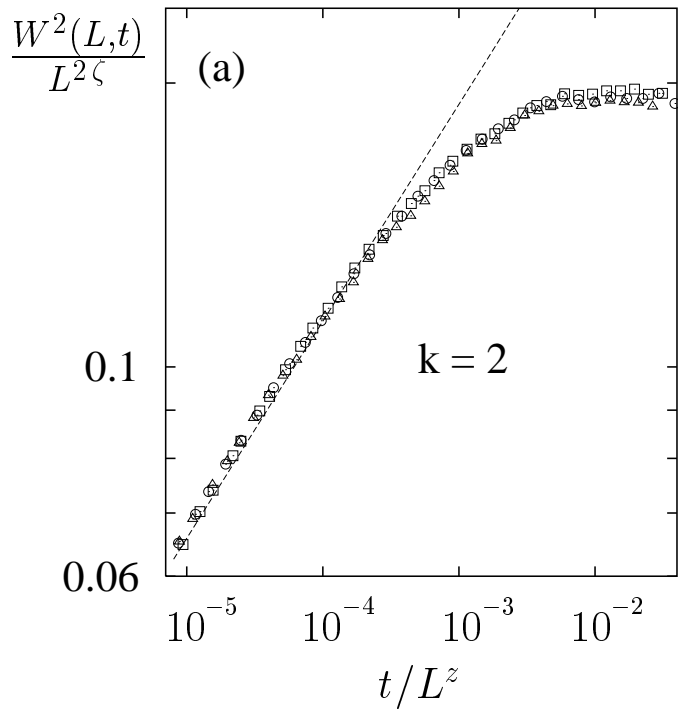


Figure 4: Growth of interface width  $W^2$  using different  $k$ -mers,  $L = 2.1 \times 10^5$  lattice sites and  $\epsilon = \epsilon'$ . For comparison, the uppermost curve shows the monomer case whereas lower curves correspond to  $k = 2, 4$ , and  $8$ , in descending order. For  $k > 1$ , straight lines are fitted with the values of  $2\beta$  given in Tab. I





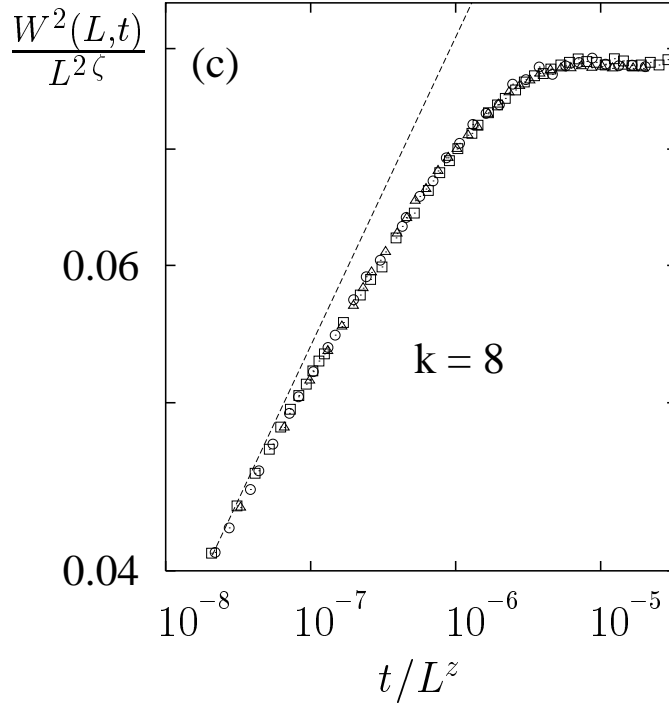


Figure 5: Finite size scaling of interface width  $W(L, t)$  using null strings and  $\epsilon = \epsilon'$  for (a)  $k = 2$ , (b)  $k = 4$  and, (c)  $k = 8$ . Sizes  $L = 400, 640,$  and,  $800$  are denoted respectively by squares, circles and triangles. The data collapse was attained upon tuning the set of exponents  $\{z, \zeta\}$  given in Table I. The straight lines are fitted with the values of  $2\beta$  obtained in the thermodynamic limit.

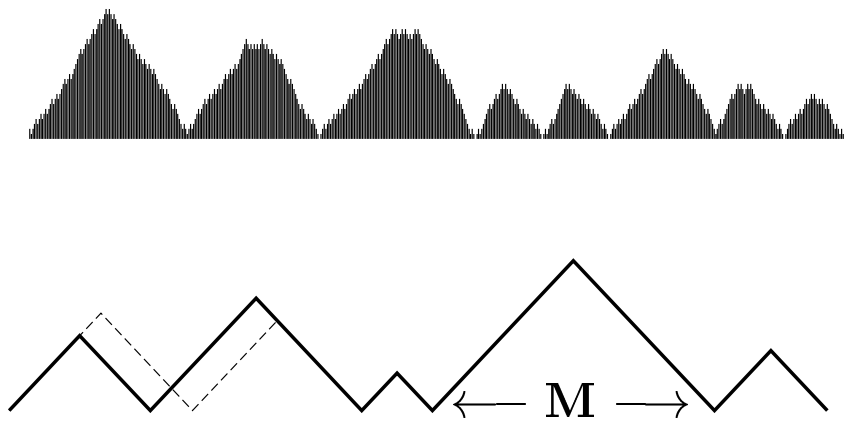


Figure 6: Evolution snapshot for dimers after  $10^4$  steps for  $\epsilon'/\epsilon = 0.4$ . Only 500 sites are shown (upper panel). The dotted lines in the schematic representation denotes the rebuilding process described in the text (lower panel).

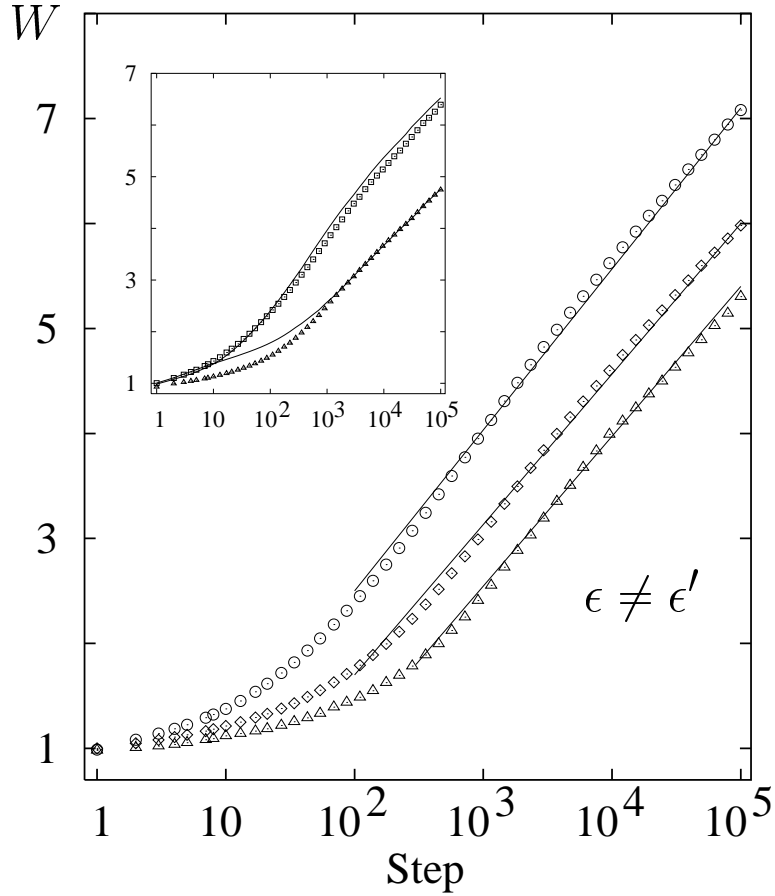


Figure 7: Logarithmic growth of the interface width for  $\epsilon'/\epsilon = 0.4$  starting from a flat substrate. Straight lines over circles ( $k = 2$ ), romboids ( $k = 4$ ), and triangles ( $k = 8$ ) are guides to the eye. The upper inset displays similar results for  $k = 2$  in sectors (3) (triangles), and (5) (squares), which are closely and respectively followed by those of sectors (4) and (2) (solid lines).